

# Distribution of Off-Diagonal Cross Sections in Quantum Chaotic Scattering: Exact Results and Data Comparison

Santosh Kumar,<sup>1,\*</sup> Barbara Dietz,<sup>2,†</sup> Thomas Guhr,<sup>3,‡</sup> and Achim Richter<sup>4,§</sup>

<sup>1</sup>*Department of Physics, Shiv Nadar University, Gautam Buddha Nagar, Uttar Pradesh 201314, India*

<sup>2</sup>*School of Physical Science and Technology, and Key Laboratory for Magnetism and Magnetic Materials of MOE, Lanzhou University, Lanzhou, Gansu 730000, China*

<sup>3</sup>*Fakultät für Physik, Universität Duisburg-Essen, Lotharstraße 1, D-47048 Duisburg, Germany*

<sup>4</sup>*Institut für Kernphysik, Technische Universität Darmstadt, D-64289 Darmstadt, Germany*

The recently derived distributions for the scattering-matrix elements in quantum chaotic systems are not accessible in the majority of experiments, whereas the cross sections are. We analytically compute distributions for the off-diagonal cross sections in the Heidelberg approach, which is applicable to a wide range of quantum chaotic systems. We thus eventually fully solve a problem which already arose more than half a century ago in compound-nucleus scattering. We compare our results with data from microwave and compound-nucleus experiments, particularly addressing the transition from isolated resonances towards the Ericson regime of strongly overlapping ones.

## I. INTRODUCTION

Scattering experiments are indispensable to understand the microscopic world. Mainly developed in nuclear physics [1–10], scattering theory now finds various applications in condensed matter physics [11–14], in classical wave systems [15–17], in wireless communication [18] and other fields [19–21]. An incoming wave in a scattering channel  $b$ , say, is modified in the scattering zone, *e.g.*, by a nucleus as the target, and leaves it through a scattering channel  $a$ . The elements  $S_{ab}(E)$  of the associated scattering matrix  $S$  are complex numbers. They provide all information on the changes in amplitude and phase, typically with energy  $E$ . The  $S$  matrix is unitary due to flux conservation and its dimension coincides with the number  $M$  of channels. In a few cases both the modulus and the phase of the  $S$ -matrix elements can be measured directly, *e.g.*, in experiments with microwave cavities, microwave networks or reverberating elastic objects [22–25]. In the majority of scattering experiments, particularly in quantum physics, the phase is not accessible. In mesoscopic quantum dots [26] the electron transport, that is, the conductance is measured instead, of which the fluctuations are well understood [13, 14, 27, 28]. In a scattering experiment involving quantum particles, *i.e.*, atoms [29–32], molecules [33, 34] or nuclei [35], only the incoming and outgoing particle current can be measured. Their ratio yields the cross sections. For  $a \neq b$  they are given by

$$\sigma_{ab}(E) = |S_{ab}(E)|^2 = (\text{Re } S_{ab}(E))^2 + (\text{Im } S_{ab}(E))^2. \quad (1)$$

This formula might have to be supplemented with multiplicative factors of purely kinematic origin.

If the dynamics in the scattering zone is sufficiently complex or, in a rather general sense, chaotic, scattering can usually be thought of as a random process [36]. There are in principle two stochastic approaches to chaotic scattering [8, 13]. In the Mexico approach [37, 38], the  $S$  matrix as a whole is viewed as a random matrix, whereas in the Heidelberg approach randomness is assumed for the Hamiltonian  $H$  describing the internal dynamics in the interaction region. While the former has an unrivaled conceptual elegance, the latter is better suited for grasping important features of the internal dynamics since the scattering process as such is fully modeled on the microscopic level.

We have three goals: First, we calculate within the Heidelberg approach the exact distribution of the off-diagonal cross sections  $\sigma_{ab}$  with  $a \neq b$ , corresponding to inelastic scattering or rearrangement collisions, thereby providing the complete solution of a long-standing problem. It applies from the regime of isolated resonances with average resonance width  $\Gamma$  smaller than the average resonance spacing  $D$ , *i.e.*,  $\Gamma/D \ll 1$ , all the way up to the Ericson regime [39] of strongly overlapping resonances,  $\Gamma/D \gg 1$ . Second, we test our results by comparing with cross-section data obtained in microwave and compound-nucleus experiments, focussing on the transition to the Ericson regime. Third, we provide a simple and robust method to extract non-random contributions to the cross-section distribution.

## II. SCATTERING MATRIX

The Heidelberg approach [40, 41] is based on [5]

$$S_{ab}(E) = \delta_{ab} - i2\pi W_a^\dagger G(E) W_b, \quad (2)$$

$$G^{-1}(E) = E\mathbf{1}_N - H + i\pi \sum_{c=1}^M W_c W_c^\dagger, \quad (3)$$

where  $G(E)$  is the matrix resolvent. The widths of the resonances generated by the poles of  $G(E)$  in the complex

\*Electronic address: skumar.physics@gmail.com

†Electronic address: dietz@lzu.edu.cn

‡Electronic address: thomas.guhr@uni-due.de

§Electronic address: richter@ikp.tu-darmstadt.de

energy plane exhibit non-trivial fluctuations [42]. They are controlled by the interplay between the Hamilton matrix  $H$  describing the scattering zone and the coupling vectors  $W_c$  which account for the interaction between the channels  $c$  and the states of  $H$ .

Scattering can involve different time scales. In nuclear physics, there are direct, non-random reactions on very short time scales due to channel-channel coupling. On longer time scales a compound nucleus is formed by the target and the incoming particles. Its equilibration ensures a sufficient amount of stochasticity, justifying the replacement of  $H$  by a random matrix. We assume absence of direct coupling between the channels, implying that the coupling vectors  $W_c$  may be chosen orthogonal,  $W_c^\dagger W_d = \gamma_c \delta_{cd}/\pi$  [41, 43] where  $\gamma_c$  is referred to as partial width. Depending on whether the system is time-reversal invariant or noninvariant,  $H$  either belongs to the Gaussian Orthogonal Ensemble (GOE) or to the Gaussian Unitary Ensemble (GUE) [8, 44] designated by the Dyson indices  $\beta = 1$  and  $\beta = 2$ , respectively. The entries of the matrices  $H$  are Gaussian distributed,  $\mathcal{P}(H)d[H] \sim \exp\left(-\frac{\beta N}{4v^2} \text{tr} H^2\right) d[H]$  with variance parameter  $v^2$ . The flat measure  $d[H]$  is the product of differentials of all independent elements in the  $N \times N$  matrix  $H$ . All physical quantities are measured on the local scale of the mean level spacing. This implies universality, *i.e.*, a very large class of probability densities gives the same result in the limit  $N \rightarrow \infty$ ; see Refs. [8, 44].

### III. CROSS-SECTION DISTRIBUTION

Although the cross-section distribution was of high interest already in the early days of compound-nucleus and, more generally, of chaotic scattering, it continued to resist an analytical solution [45]. In a seminal work using the supersymmetry method, Verbaarschot, Weidenmüller and Zirnbauer [40] derived the exact two-point energy correlation function of the  $S$ -matrix elements. Davis and Boosé calculated three- and four-point correlation functions [46, 47] and Fyodorov, Savin and Sommers the distribution of the diagonal  $S$ -matrix elements [48]. Rozhkov, Fyodorov, and Weaver [49, 50] computed a related quantity, namely the statistics of transmitted power. Putting forward a new variant of the supersymmetry method, we recently calculated the distributions of the real and the imaginary parts of the off-diagonal  $S$  matrix [51, 52]. In a related study, Fyodorov and Nock obtained the distributions of off-diagonal elements of the Wigner  $K$  matrix [53]. Nevertheless, the cross-section distribution remained out of reach, because the cross section (1) depends on the real and imaginary parts of the  $S$ -matrix element which are not independent. Thus, to compute it for  $a \neq b$ ,

$$p(\sigma_{ab}) = \int_{-\infty}^{\infty} dx_1 \int_{-\infty}^{\infty} dx_2 \delta(\sigma_{ab} - x_1^2 - x_2^2) P(x_1, x_2), \quad (4)$$

the knowledge of the joint probability density function

$$P(x_1, x_2) = \int d[H] \mathcal{P}(H) \delta(x_1 - \text{Re } S_{ab}) \delta(x_2 - \text{Im } S_{ab}) \quad (5)$$

is inevitable. At first sight, one might expect that this task leads to doubling the size of the supersymmetric non-linear sigma model as compared to Refs. [48, 51, 52], rendering further evaluation forbiddingly complicated. However, we recently discovered that a simple, yet far-reaching modification and generalization of our supersymmetry technique in Refs. [51, 52] yields  $P(x_1, x_2)$  without enlarging this size.

### IV. JOINT PROBABILITY DENSITY

It turns out to be advantageous to employ the Fourier transform, *i.e.*, the bivariate characteristic function

$$R(k_1, k_2) = \int d[H] \mathcal{P}(H) e^{-ik_1 \text{Re } S_{ab} - ik_2 \text{Im } S_{ab}} \quad (6)$$

in two dimensions, such that

$$P(x_1, x_2) = \frac{1}{4\pi^2} \int_{-\infty}^{\infty} dk_1 \int_{-\infty}^{\infty} dk_2 e^{ik_1 x_1 + ik_2 x_2} R(k_1, k_2). \quad (7)$$

Anticipating the data analysis to follow we emphasize that the characteristic function is obtained by sampling from the experimental data as easily as the joint probability density itself. With Eq. (7) in Eq. (4) and the complex variables  $\mathbf{k} = k_1 + ik_2$  and  $\mathbf{x} = x_1 + ix_2$ , we find

$$p(\sigma_{ab}) = \frac{1}{4\pi^2} \int d^2 \mathbf{x} \int d^2 \mathbf{k} \delta(\sigma_{ab} - |\mathbf{x}|^2) e^{i \text{Re}(\mathbf{k}^* \mathbf{x})} R(\mathbf{k}). \quad (8)$$

The  $\mathbf{x}$  integrals can be done with polar coordinates,

$$p(\sigma_{ab}) = \frac{1}{4\pi} \int d^2 \mathbf{k} R(\mathbf{k}) J_0(\sqrt{\sigma_{ab}} |\mathbf{k}|), \quad (9)$$

expressing the cross-section distribution as a certain Bessel transform of the characteristic function. The crucial step to make the calculation of the latter feasible is to use Eq. (3) in Eq. (6) in the form

$$R(\mathbf{k}) = \int d[H] \mathcal{P}(H) \exp(-i\pi W^T A W) \quad (10)$$

with the  $2N$  component vector  $W^T = [W_a^T, W_b^T]$  for  $a \neq b$ , and the  $2N \times 2N$  Hermitian matrix

$$A = \begin{bmatrix} 0 & -i\mathbf{k}^* G \\ i\mathbf{k} G^\dagger & 0 \end{bmatrix} \quad (11)$$

in terms of the resolvent in Eq. (3). In Refs. [51, 52] we proceeded similarly, but for marginal distributions and thus univariate characteristic functions that depend either on  $k_1$  or on  $k_2$ . Absorbing them as complex variable  $\mathbf{k}$  into the definition of  $A$  preserves its Hermiticity.

Hence, we may adjust all further steps in Refs. [51, 52] by moving the calculation into the complex  $\mathbf{k}$  plane. We introduce bosonic integrals for a Fourier transform of the characteristic function (10) in  $W$  space to invert the resolvent  $G$  in  $A$ . A thereby occurring determinant is written as a fermionic integral. This allows us to do the ensemble average over the random matrices  $H$  exactly. We obtain a supermatrix model that we bring onto the local scale by a saddlepoint approximation for  $N \rightarrow \infty$ . This yields a supersymmetric nonlinear sigma model extending the one in Refs. [51, 52]. Details are given in Sect. I of the appendix Sec. VIII.

For  $\beta = 2$  with unitarily invariant  $H$  the final result for the characteristic function is

$$R(\mathbf{k}) = 1 - \int_1^\infty d\lambda_1 \int_{-1}^1 d\lambda_2 \frac{|\mathbf{k}|^2}{4(\lambda_1 - \lambda_2)^2} \mathcal{F}_U(\lambda_1, \lambda_2) \times (t_a^1 t_b^1 + t_a^2 t_b^2) J_0 \left( |\mathbf{k}| \sqrt{t_a^1 t_b^1} \right), \quad (12)$$

with the channel factor

$$\mathcal{F}_U(\lambda_1, \lambda_2) = \prod_{c=1}^M \frac{g_c^+ + \lambda_2}{g_c^+ + \lambda_1}, \quad (13)$$

where  $t_c^j = \sqrt{|\lambda_j^2 - 1|/(g_c^+ + \lambda_j)}$ , and  $g_c^\pm = (v^2 \pm \gamma_c^2)/(\gamma_c \sqrt{4v^2 - E^2})$ . The parameter  $g_c^+$  is related to the transmission coefficient or the sticking probability  $T_c = 1 - |S_{cc}|^2$  as  $g_c^+ = 2/T_c - 1$ . The remarkable fact that the characteristic function (12) depends only on  $|\mathbf{k}|$  implies that the distribution of real and imaginary parts of  $S_{ab}$  are identical [51, 52] for  $\beta = 2$ . For  $\beta = 1$  with orthogonally invariant  $H$  we arrive at

$$R(\mathbf{k}) = 1 + \frac{1}{8\pi} \int_{-1}^1 d\lambda_0 \int_1^\infty d\lambda_1 \int_1^\infty d\lambda_2 \int_0^{2\pi} d\psi \times \mathcal{J}(\lambda_0, \lambda_1, \lambda_2) \mathcal{F}_O(\lambda_0, \lambda_1, \lambda_2) (\kappa_1 + \kappa_2 + \kappa_3 + \kappa_4). \quad (14)$$

The Jacobian in the above expression is given by

$$\mathcal{J} = \frac{(1 - \lambda_0^2)|\lambda_1 - \lambda_2|}{2(\lambda_1^2 - 1)^{1/2}(\lambda_2^2 - 1)^{1/2}(\lambda_1 - \lambda_0)^2(\lambda_2 - \lambda_0)^2}, \quad (15)$$

and the channel factor reads

$$\mathcal{F}_O(\lambda_0, \lambda_1, \lambda_2) = \prod_{c=1}^M \frac{g_c^+ + \lambda_0}{(g_c^+ + \lambda_1)^{1/2}(g_c^+ + \lambda_2)^{1/2}}. \quad (16)$$

The  $\kappa$ 's in Eq. (14) depend on  $g_c^\pm$  and the complex  $\mathbf{k}$  in a nontrivial way; see Sec. VIII.

## V. COMPARISON WITH MICROWAVE DATA

The mathematical equivalence of spectra of two-dimensional quantum billiards and flat microwave resonators is used to experimentally explore a variety of

quantum chaotic phenomena in closed [22, 23, 54, 55] and open systems [56–62]. Here, we use the data measured for a microwave billiard in the shape of a classically chaotic tilted-stadium billiard; see Refs. [61–63] for experimental details. The  $S$ -matrix elements  $S_{ab}$  were measured in steps of 100 kHz in a range from 1 to 25 GHz. Their fluctuation properties were evaluated in frequency windows of 1 GHz to guarantee a negligible secular variation of the coupling vectors  $W_c$ . In Ref. [51] we analyzed the marginal distributions of real and imaginary parts of  $S_{ab}$  and the corresponding univariate characteristic functions separately. We now compare our new analytical results for the joint probability density  $P(x_1, x_2)$ , for the bivariate characteristic function  $R(k_1, k_2)$  and for the cross section distribution  $p(\sigma_{ab})$  with these data. Figure 1 shows the bivariate characteristic function in the frequency range 10–11 GHz. Plotted are the analytical and experimental results together. The same comparison is shown in Fig. 2 for the frequency range 24–25 GHz; see also Sec. VIII. The agreement is very good in

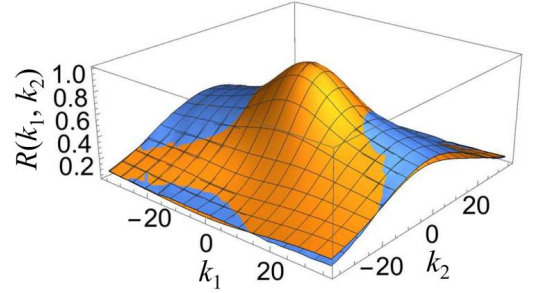


FIG. 1: Bivariate characteristic function  $R(k_1, k_2)$  in the frequency range 10–11 GHz. Analytical result (blue) and microwave data (orange).

both cases. For the lower frequencies, the peak is broad and heavy-tailed, corresponding to a non-Gaussian joint probability density. For the higher ones, the peak is narrow and Gaussian-like, yielding the joint probability density with a nearly Gaussian shape for the frequency range 24–25 GHz, displayed in Fig. 8. To explain these results, we point out that the system undergoes with increasing frequency a transition from isolated resonances to largely

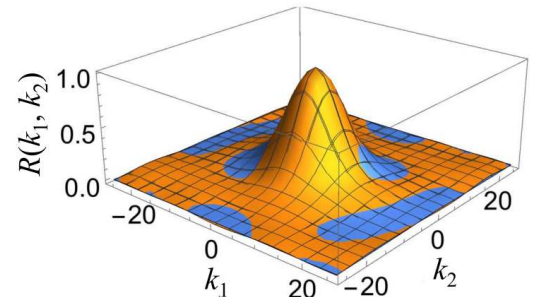


FIG. 2: As Fig. 1, but in the frequency range 24–25 GHz.

overlapping ones, *i.e.*, to the onset region of the Ericson regime [63]. For the frequency ranges 10-11 GHz and 24-25 GHz, we have  $\Gamma/D = 0.23$  and  $\Gamma/d = 1.21$ , respectively. In the Ericson regime, scattering matrices and cross sections are random functions and the peaks in the spectra cannot be associated with particular resonances, implying that the distribution of the  $S$ -matrix elements is Gaussian [3, 41]. According to Eq. (4), the distribution of normalized cross sections is then exponential with  $p(0) = 1$ . To test this, we also compare in Fig. 4 our results for the distribution of cross sections normalized to their mean with the data. As seen, our exact results compare well to all regimes including the transition region. The nearly exponential form with  $p(0) > 1$  in the frequency range 24-25 GHz clearly indicates that we are in the onset of the Ericson regime.

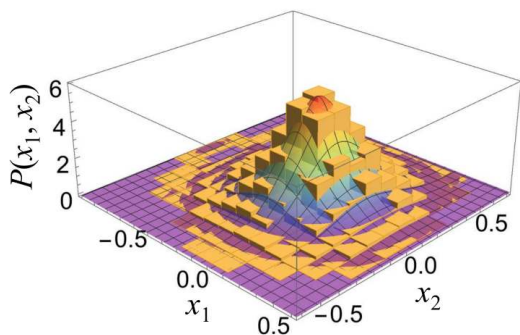


FIG. 3: Joint probability density  $P(x_1, x_2)$ , analytical (surface) and microwave data (histogram) in the frequency range 24-25 GHz.

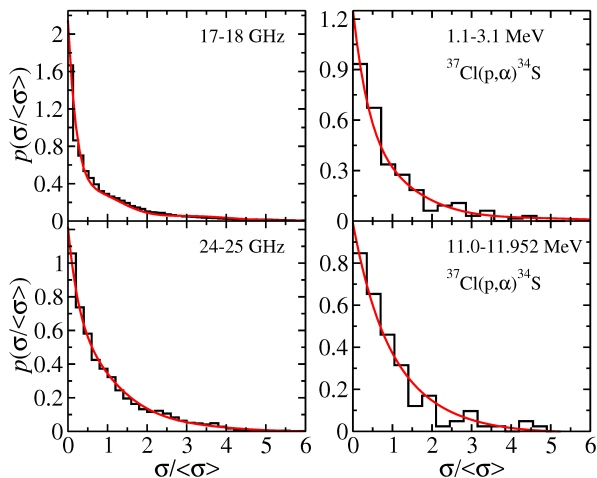


FIG. 4: Distribution of normalized cross sections. Experimental data as histograms from microwave (left) and nuclear experiments (right), respectively. Analytical results as solid red lines.

## VI. COMPARISON WITH COMPOUND-NUCLEUS DATA

We also use data from historical measurements of the compound-nuclear reaction  $^{37}\text{Cl}(p, \alpha)^{34}\text{S}$  [64–66]. In Ref. [65], excitation functions were measured in steps of 8 keV in the proton-energy range 11-11.952 MeV for 12 scattering angles between  $31^\circ$  to  $175^\circ$ . Importantly, these data are fully in the Ericson regime with  $\Gamma/D \approx 27 - 36$ . In Fig. 5 we show a selection of three such excitation functions for  $31^\circ$ ,  $110^\circ$  and  $175^\circ$ . At smaller angles, one observes a background, *i.e.*, a nonzero minimum value of the excitation function. It is due to direct reactions, in which, *e.g.*, an incoming particle kicks out an  $\alpha$  particle without formation of a compound nucleus. As such processes are stronger in forward than in backward direction, the background disappears at larger angles. In addition, they are barely affected by the chaotic dynamics in the scattering zone and thus cannot be random. Hence, their energy dependence is marginal and we may safely subtract the background to obtain the fluctuating compound-nuclear contribution. In Fig. 4 we compare the distribution of normalized cross-sections, *i.e.*,  $p(\sigma/\langle\sigma\rangle)$  obtained from the  $175^\circ$  measurement with the analytical prediction. For this, we use  $M = 5$  (effective) open channels and all transmission coefficients  $T_c = 0.99$  in accordance with Ref. [65], leading to an exponential. We find a very good match.

To complete our studies we, furthermore, apply our analytical results to nuclear data in the region of weakly overlapping resonances. In Ref. [67], the reaction  $^{37}\text{Cl}(p, \alpha)^{34}\text{S}$  was measured in the proton-energy range 1.1-3.1 MeV at a scattering angle of  $90^\circ$ . These data, shown in Fig. 6, exhibit an unusually sharp increase at an energy of approximately 2.6 MeV which is due to experimental imperfections. We thus restrict the data analysis to the energy range 1.1-2.6 MeV. The background stemming from the direct reactions is a smoothly increasing function of energy, hence subtracting it is more involved than in the previously considered case; see Fig. 5. This reflects a general problem in analyzing compound-nuclear data. Unfortunately, we cannot exploit recent progress that has been made employing the  $K$  matrix [68, 69], since it relies on the knowledge of the  $S$ -matrix elements. Instead, we put forward a seemingly new empirical method which is based on the observation that the peak exhibited by the cross-section distribution of compound-nuclear reactions at  $\sigma = 0$  is shifted to a nonzero value by direct contributions. Thus, we fit the excitation function below 2.6 MeV with a second-order polynomial, which we then subtract from the data. This leads to the experimental cross-section distribution displayed in Fig. 4 which is peaked at zero. Our analytical result is very well capable of describing this clearly non-exponential distribution for  $M = 10$  effective channels and  $T_c = 0.7$ .

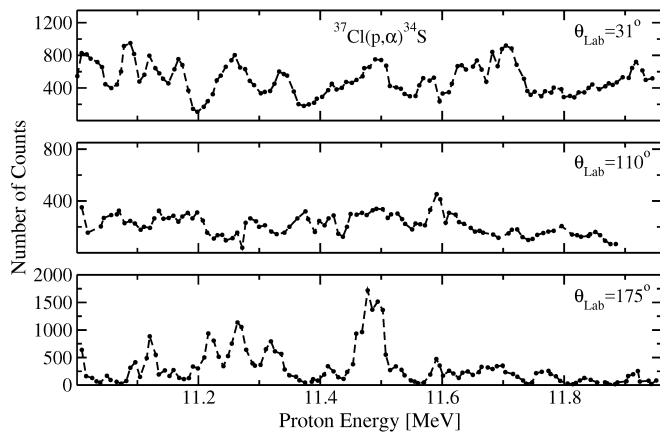


FIG. 5: Excitation functions for the reaction  $^{37}\text{Cl}(p,\alpha)^{34}\text{S}$  in the Ericson regime for scattering angles  $31^\circ$ ,  $110^\circ$  and  $175^\circ$  from top to bottom. Digitized from Ref. [65].

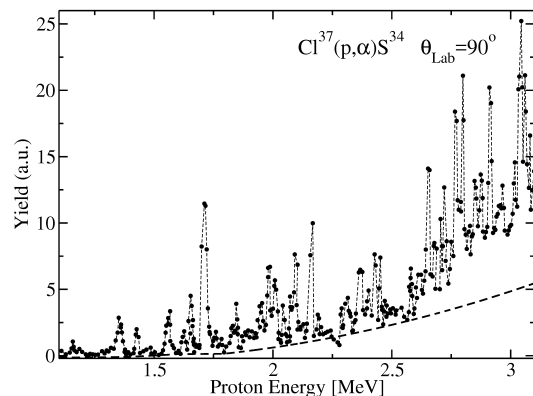


FIG. 6: Excitation functions for the reaction  $^{37}\text{Cl}(p,\alpha)^{34}\text{S}$  below the Ericson regime for scattering angle  $90^\circ$ . Digitized from Ref. [67].

## VII. CONCLUSIONS

We solved a long-standing problem by exactly calculating the distribution of the off-diagonal cross sections within the Heidelberg approach. This facilitates, for the first time, an analysis of distributions for the large number of systems, in which only the cross sections can be measured. We performed a detailed comparison with microwave and nuclear data, focusing on the transition from the regime of isolated resonances towards the Ericson regime. Our analytical results describe the data very well in all regimes. We are not aware of any comparable study for distributions and characteristic functions. In the course of our data comparison, we came up with a seemingly new and robust method to subtract the direct part in cross-section data which only relies on experimental information.

## Acknowledgments

We are grateful to A. Nock for his help in the initial stages of this project, and to P. von Neumann-Cosel who helped us to find Ref. [67]. We acknowledge fruitful discussions with T. Kawano and H.A. Weidenmüller. SK also acknowledges the support by the grant EMR/2016/000823 provided by SERB, DST, Government of India. This work was supported by the Deutsche Forschungsgemeinschaft (DFG) within the Collaborative Research Centers 634 and 1245.

- 
- [1] T. E. O. Ericson, Ann. Phys. (NY) **23**, 390 (1963).
  - [2] G. R. Satchler, Phys. Letters **7**, 55 (1963).
  - [3] D. M. Brink and R. O. Stephen, Phys. Lett. **5**, 77 (1963).
  - [4] C. E. Porter, *Statistical Theories of Spectra: Fluctuations* (Academic, New York, 1965).
  - [5] C. Mahaux and H.A. Weidenmüller, *Shell Model Approach to Nuclear Reactions* (North Holland, Amsterdam, 1969).
  - [6] H. Feshbach, *Nuclear Reactions* (Wiley Classics Library, NY, 1993).
  - [7] V. Zelevinsky, Annu. Rev. Nucl. Part. Sci. **46**, 237 (1996).
  - [8] T. Guhr, A. Müller-Groeling, H. A. Weidenmüller, Phys. Rep. **299** (1998) 189.
  - [9] R. Pike, P. Sabatier (Eds.), *Scattering and Inverse Scattering in Pure and Applied Sciences* (Academic Press, New York, 2002).
  - [10] H. A. Weidenmüller and G. Mitchell, Rev. Mod. Phys. **81**, 539 (2009).
  - [11] P. A. Lee, A. Douglas Stone, and H. Fukuyama, Phys. Rev. B **35**, 1039 (1987).
  - [12] R. A. Jalabert, H. U. Baranger, and A. Douglas Stone, Phys. Rev. Lett. **65**, 2442 (1990).
  - [13] C. W. Beenakker, Rev. Mod. Phys. **69**, 731 (1997).
  - [14] Y. Alhassid, Rev. Mod. Phys. **69** 72, 895 (2000).
  - [15] R. L. Weaver, J. Acoust. Soc. Am. **85**, 1005 (1989).
  - [16] C. Ellegaard, T. Guhr, K. Lindemann, H. Q. Lorensen, J. Nygård, and M. Oxenford, Phys. Rev. Lett. **75**, 1546 (1995).
  - [17] J.-B. Gros, O. Legrand, F. Mortessagne, E. Richalot, and K. Selezmani, Wave Motion **51**, 664 (2014).
  - [18] R. Couillet and M. Debbah, *Random Matrix Methods for Wireless Communications* (Cambridge University Press, Cambridge, 2011).
  - [19] Y.V. Fyodorov, T. Kottos, H.-J. Stöckmann, J. Phys. A: Math. Gen. **38** (2005).
  - [20] G. E. Mitchell, A. Richter, and H. A. Weidenmüller, Rev. Mod. Phys. **82**, 2845 (2010).
  - [21] J.-H. Yeh, T. M. Antonsen, E. Ott, and S. M. Anlage, Phys. Rev. E **85**, 015202 (2012).
  - [22] H.-J. Stöckmann and J. Stein, Phys. Rev. Lett. **64**, 2215

- (1990).
- [23] H.-D. Gräf, H. L. Harney, H. Lengeler, C. H. Lewenkopf, C. Rangacharyulu, A. Richter, P. Schardt, and H. A. Weidenmüller, *Phys. Rev. Lett.* **69**, 1296 (1992).
  - [24] O. Hul, S. Bauch, P. Pakoński, N. Savytsky, K. Życzkowski, and L. Sirko, *Phys. Rev. E* **69**, 056205 (2004).
  - [25] M. Avlund, C. Ellegaard, M. Oxborrow, T. Guhr, and N. Søndergaard, *Phys. Rev. Lett.* **104**, 164101 (2010).
  - [26] J. A. Folk, S. R. Patel, S. F. Godijn, A. G. Huibers, S. M. Cronenwett, and C. M. Marcus, *Phys. Rev. Lett.* **76**, 1699 (1996).
  - [27] H. A. Weidenmüller, *Nucl. Phys.* **A518**, 1 (1990).
  - [28] G. L. Celardo, F. M. Izrailev, S. Sorathia, V. G. Zelevinsky, and G. P. Berman, *AIP Conf. Proc.* **995**, 75 (2008).
  - [29] Jörg Main and Günter Wunner, *Phys. Rev. Lett.* **69**, 586 (1992).
  - [30] G. Stania and H. Walther, *Phys. Rev. Lett.* **95**, 194101 (2005).
  - [31] J. Madroñero and A. Buchleitner, *Phys. Rev. Lett.* **95**, 263601 (2005).
  - [32] A. Frisch, M. Mark, K. Aikawa, F. Ferlino, J. L. Bohn, C. Makrides, A. Petrov, and S. Kotochigova, *Nature (London)* **507**, 475 (2014).
  - [33] S. A. Reid and H. Reisler, *J. Chem. Phys.* **100**, 474 (1996).
  - [34] M. Mayle, G. Quémener, B. P. Ruzic, and J. L. Bohn, *Phys. Rev. A* **87**, 012709 (2013).
  - [35] T. E. O. Ericson and T. Mayer-Kuckuk, *Annu. Rev. Nucl. Sci.* **16**, 183 (1966).
  - [36] C. Jung, T. H. Seligman, *Phys. Rep.* **285**, 77 (1997).
  - [37] P. A. Mello, P. Pereya, and T. H. Seligman, *Ann. Phys.* **161**, 254 (1985).
  - [38] M. Martínez-Mares and P. A. Mello, *Phys. Rev. E* **72**, 026224 (2005).
  - [39] T. E. O. Ericson, *Phys. Rev. Lett.* **5**, 430 (1960).
  - [40] J. J. M. Verbaarschot, H. A. Weidenmüller and M. R. Zirnbauer, *Phys. Rep.* **129**, 367 (1985).
  - [41] D. Agassi, H. A. Weidenmüller, G. Mantzouranis, *Phys. Rep.* **22**, 145 (1975).
  - [42] Y. V. Fyodorov and H.-J. Sommers, *J. Math. Phys.* **38**, 1918 (1997).
  - [43] C. H. Lewenkopf, H. A. Weidenmüller, *Ann. Phys.* **212**, 53 (1991).
  - [44] M. L. Mehta, *Random Matrices* (New York: Academic Press, 2004).
  - [45] T. E. O. Ericson, B. Dietz, and A. Richter, *Phys. Rev. E* **94**, 042207 (2016).
  - [46] E. D. Davis, D. Boosé, *Phys. Lett. B* **211**, 379 (1988).
  - [47] E. D. Davis, D. Boosé, *Z. Phys. A* **332**, 427 (1989).
  - [48] Y. V. Fyodorov, D. V. Savin, and H.-J. Sommers, *J. Phys. A* **38**, 10731 (2005).
  - [49] I. Rozhkov, Y. V. Fyodorov, and R. L. Weaver, *Phys. Rev. E* **68**, 016204 (2003).
  - [50] I. Rozhkov, Y. V. Fyodorov, and R. L. Weaver, *Phys. Rev. E* **69**, 036206 (2004).
  - [51] S. Kumar, A. Nock, H.-J. Sommers, T. Guhr, B. Dietz, M. Miski-Oglu, A. Richter, and F. Schäfer, *Phys. Rev. Lett.* **111**, 030403 (2013).
  - [52] A. Nock, S. Kumar, H.-J. Sommers, and T. Guhr, *Ann. Phys.* **342**, 103 (2014).
  - [53] Y. V. Fyodorov and A. Nock, *J. Stat. Phys.* **159**, 731 (2015).
  - [54] S. Sridhar, *Phys. Rev. Lett.* **67**, 785 (1991).
  - [55] B. Dietz and A. Richter, *CHAOS* **25**, 097601 (2015).
  - [56] U. Kuhl, M. Martínez-Mares, R. A. Méndez-Sánchez, and H.-J. Stöckmann, *Phys. Rev. Lett.* **94**, 144101 (2005).
  - [57] U. Kuhl, H.-J. Stöckmann, and R. Weaver, *J. Phys. A: Math. Gen.* **38**, 10433 (2005).
  - [58] S. Hemmady, X. Zheng, T. M. Antonsen, E. Ott, and S. M. Anlage, *Phys. Rev. E* **71**, 056215 (2005).
  - [59] O. Hul, O. Tymoshchuk, S. Bauch, P. M. Koch, and L. Sirko, *J. Phys. A: Math. Gen.* **38**, 10489 (2005).
  - [60] M. Lawniczak, O. Hul, S. Bauch, P. Sēba, and L. Sirko, *Phys. Rev. E* **77**, 056210 (2008).
  - [61] B. Dietz, T. Friedrich, H. L. Harney, M. Miski-Oglu, A. Richter, F. Schäfer, J. Verbaarschot, and H. A. Weidenmüller, *Phys. Rev. Lett.* **103**, 064101 (2009).
  - [62] B. Dietz, T. Friedrich, H. L. Harney, M. Miski-Oglu, A. Richter, F. Schäfer, and H. A. Weidenmüller, *Phys. Rev. E* **81**, 036205 (2010).
  - [63] B. Dietz, H. L. Harney, A. Richter, F. Schäfer, and H. A. Weidenmüller, *Phys. Lett. B* **685**, 263 (2010).
  - [64] P. von Brentano, J. Ernst, O. Häusser, T. Mayer-Kuckuk, A. Richter, and W. von Witsch, *Phys. Lett.* **9**, 48 (1964).
  - [65] W. von Witsch, P. von Brentano, T. Mayer-Kuckuk, and A. Richter, *Nucl. Phys.* **80**, 394 (1966).
  - [66] A. Richter, A. Bamberger, P. von Brentano, T. Mayer-Kuckuk, and W. von Witsch, *Z. Naturforsch.* **21a**, 1001 (1966).
  - [67] R. L. Clarke, E. Almqvist, and E. B. Paul, *Nucl. Phys.* **14**, 472 (1959).
  - [68] T. Kawano, P. Talou, and H. A. Weidenmüller, *Phys. Rev. C* **92**, 044617 (2015).
  - [69] T. Kawano, R. Capore, S. Hilaire, and P. Chau Huu-Tai, *Phys. Rev. C* **94**, 014612 (2016).

## VIII. APPENDIX

### Appendix A: Derivation of the characteristic functions for the cases $\beta = 1, 2$

Although the derivation to follow can be, with the necessary adjustments, inferred from Refs. [51, 52], we document here the crucial steps for the readers less experienced with supersymmetry calculations. For the case of unitarily invariant  $H$ , i.e.  $\beta = 2$ , in order to bring the matrix  $A$  into a diagonal form, we consider the following transformations:

$$z \rightarrow \Xi_z z, \quad z^\dagger \rightarrow z^\dagger, \quad \zeta \rightarrow \Xi_\zeta \zeta, \quad \zeta^\dagger \rightarrow \zeta^\dagger \quad (\text{A1})$$

with

$$\Xi_z = \begin{bmatrix} 0 & -i\mathbf{k}^* \\ -i\mathbf{k} & 0 \end{bmatrix} \otimes \mathbb{1}_N, \quad \Xi_\zeta = \begin{bmatrix} 0 & i\mathbf{k}^* \\ -i\mathbf{k} & 0 \end{bmatrix} \otimes \mathbb{1}_N. \quad (\text{A2})$$

The characteristic function, therefore, can be written as

$$R(\mathbf{k}) = (-1)^N \int d[H] \mathcal{P}(H) \int d[\Psi] e^{\frac{i}{2}(\mathbf{U}^\dagger \Psi + \Psi^\dagger \mathbf{W}) + \frac{i}{4\pi} \Psi^\dagger \mathcal{A}^{-1} \Psi}, \quad (\text{A3})$$

where

$$\mathcal{A}^{-1} = \text{diag} [-(G^{-1})^\dagger, G^{-1}, -(G^{-1})^\dagger, -G^{-1}] \quad (\text{A4})$$

is a block diagonal  $4N \times 4N$  matrix which is independent of  $\mathbf{k}$ . Also

$$\mathbf{U}^T = [i\mathbf{k}^* W_b^T, i\mathbf{k} W_a^T, 0, 0], \quad \mathbf{W}^T = (1/2)[W_a^T, W_b^T, 0, 0] \quad (\text{A5})$$

are  $4N$ -dimensional vectors composed of the coupling vectors. Apart from the expressions of  $\mathbf{U}$  and  $\mathbf{W}$ , the characteristic function for the joint probability distribution  $\mathcal{P}(H)$  has the same form as that for the joint probability distribution of the real and imaginary parts of  $S$ , compare with Eq. (11) of Ref. [51] and Eq. (21) of Ref. [52]. In particular, the definition of  $\mathcal{A}^{-1}$  is exactly the same. This allows us to proceed as in Refs. [51, 52], leading to an exact representation of the characteristic function for arbitrary  $N$  in terms of a matrix integral in superspace:

$$\begin{aligned} R(\mathbf{k}) &= \int d[\tau] e^{-\frac{4\pi^2 N}{v^2} \text{str } \tau^2 - \frac{i}{4} \mathbf{U}^\dagger (\mathbf{L}^{1/2} \mathcal{T} \mathbf{L}^{1/2})^{-1} \mathbf{W} \text{sdet}^{-1} \mathcal{T}}, \\ \mathcal{T} &= \tau_E \otimes \mathbb{1}_N + \frac{i}{4} L \otimes \sum_{c=1}^M W_c W_c^T, \quad \tau_E = \tau - \frac{E}{4\pi} \mathbb{1}_4, \\ L &= \text{diag}(+1, -1, +1, -1), \quad \mathbf{L} = L \otimes \mathbb{1}_N. \end{aligned} \quad (\text{A6})$$

Here “str” and “sdet” denote the supertrace and superdeterminant, respectively. The supermatrix integral can be performed using saddle-point analysis in the  $N \rightarrow \infty$  limit, thereby mapping it to a nonlinear sigma model. By employing the standard parametrization as in [51, 52], we obtain the final expression Eq. (13) for the characteristic function in the  $\beta = 2$  case.

We now focus on the orthogonally invariant  $H$ , *i.e.*,  $\beta = 1$  and instead of the transformation given in Eq. (18) we implement the following one:

$$z \rightarrow \Xi_z z, \quad z^\dagger \rightarrow z^\dagger \Xi_{z^\dagger}, \quad \zeta \rightarrow \Xi_\zeta \zeta, \quad \zeta^\dagger \rightarrow \zeta^\dagger \Xi_{\zeta^\dagger} \quad (\text{A7})$$

with

$$\begin{aligned} \Xi_z &= \begin{bmatrix} 0 & \sqrt{-i\mathbf{k}^*} \\ \sqrt{-i\mathbf{k}} & 0 \end{bmatrix} \otimes \mathbb{1}_N, \\ \Xi_{z^\dagger} &= \begin{bmatrix} 0 & \sqrt{2i\mathbf{k}^*} \\ \sqrt{-2i\mathbf{k}} & 0 \end{bmatrix} \otimes \mathbb{1}_N, \\ \Xi_\zeta &= \begin{bmatrix} \sqrt{-i\mathbf{k}} & 0 \\ 0 & \sqrt{-i\mathbf{k}^*} \end{bmatrix} \otimes \mathbb{1}_N, \\ \Xi_{\zeta^\dagger} &= \begin{bmatrix} \sqrt{-2i\mathbf{k}} & 0 \\ 0 & \sqrt{2i\mathbf{k}^*} \end{bmatrix} \otimes \mathbb{1}_N. \end{aligned}$$

We furthermore consider the supervector  $\Psi^T = [x_a^T, y_a^T, x_b^T, y_b^T, \zeta_a^T, \zeta_a^\dagger, \zeta_b^T, \zeta_b^\dagger]$ , where we decomposed  $z = x + iy$  into its real and imaginary part. This yields for the characteristic function

$$R(\mathbf{k}) = (-1)^N \int d[H] \mathcal{P}(H) \int d[\Psi] e^{i\Psi^\dagger \mathbf{V} e^{\frac{i}{4\pi} \Psi^\dagger \mathcal{A}^{-1} \Psi}}, \quad (\text{A8})$$

where

$$\mathcal{A}^{-1} = \text{diag} [-(G^{-1})^\dagger, G^{-1}, -(G^{-1})^\dagger, -G^{-1}] \otimes \mathbb{1}_2 \quad (\text{A9})$$



is a block diagonal  $8N \times 8N$  matrix which is independent of  $\mathbf{k}$ , and

$$\mathbf{V}^T = (1/2)[\sqrt{-i\mathbf{k}}(W_a + W_b)^T, -\sqrt{-i\mathbf{k}}(W_a - W_b)^T, \sqrt{-i\mathbf{k}^*}(W_a + W_b)^T, i\sqrt{-i\mathbf{k}^*}(W_a - W_b)^T, 0, 0, 0, 0] \quad (\text{A10})$$

is a  $\mathbf{k}$ -dependent  $8N$ -dimensional vector composed of the coupling vectors. It should be noted that in order to render  $\mathcal{A}^{-1}$  block-diagonal and independent of  $\mathbf{k}$ , already transforming  $z$  and  $\zeta$  omitting the square-roots in the transformation-matrices  $\Xi_z(\mathbf{k}), \Xi_\zeta(\mathbf{k})$  in Eq. (A7) would have been sufficient. However, transforming also  $z^\dagger, \zeta^\dagger$  along with  $z, \zeta$  has the advantage that the ensuing expression for  $\mathbf{V}$  becomes simpler and numerically stable. Apart from the expression of  $\mathbf{V}$ , the characteristic function for the joint probability distribution has, as in the case  $\beta = 2$ , exactly the same form as that for the joint probability distribution of the real- or imaginary part of  $S$ , compare with Eq. (12) of Ref. [51] and Eq. (70) of Ref. [52]. In particular, the definition of  $\mathcal{A}^{-1}$  is exactly the same. This allows us to perform the same computations as in the previous works, leading to an exact representation of the characteristic function for arbitrary  $N$  in terms of a matrix integral in superspace,

$$\begin{aligned} R(\mathbf{k}) &= \int d[\tau] e^{-\frac{4\pi^2 N}{v^2} \text{str } \tau^2 - \frac{i}{4} \mathbf{V}^T (\mathbf{L}^{1/2} \tau \mathbf{L}^{1/2})^{-1} \mathbf{V}} \text{sdet}^{-1/2} \mathcal{T}, \\ \mathcal{T} &= \tau_E \otimes \mathbb{1}_N + \frac{i}{4} L \otimes \sum_{c=1}^M W_c W_c^T, \quad \tau_E = \tau - \frac{E}{4\pi} \mathbb{1}_8, \\ L &= \text{diag}(+1, -1, +1, -1) \otimes \mathbb{1}_2, \quad \mathbf{L} = L \otimes \mathbb{1}_N. \end{aligned} \quad (\text{A11})$$

Here  $\tau$  is an  $8 \times 8$  dimensional supermatrix of appropriate symmetry. Again, considering the large  $N$  limit and using the standard parametrization for the supermatrix and performing the steps outlined in [52], we obtain the final result Eq. (15). In the top figures of Fig. 7 we compare our new analytical results for the bivariate characteristic function  $R(k_1, k_2)$  with those for microwave data in the frequency ranges 10-11 GHz (left), 17-18 GHz (middle) and 24-25 GHz (right). The lower figures show the difference between the analytical and the experimental results. In Fig. 8 we compare the corresponding analytical and experimental results for the joint probability density  $P(x_1, x_2)$  in the frequency ranges 17-18 GHz (left) and 24-25 GHz (right).

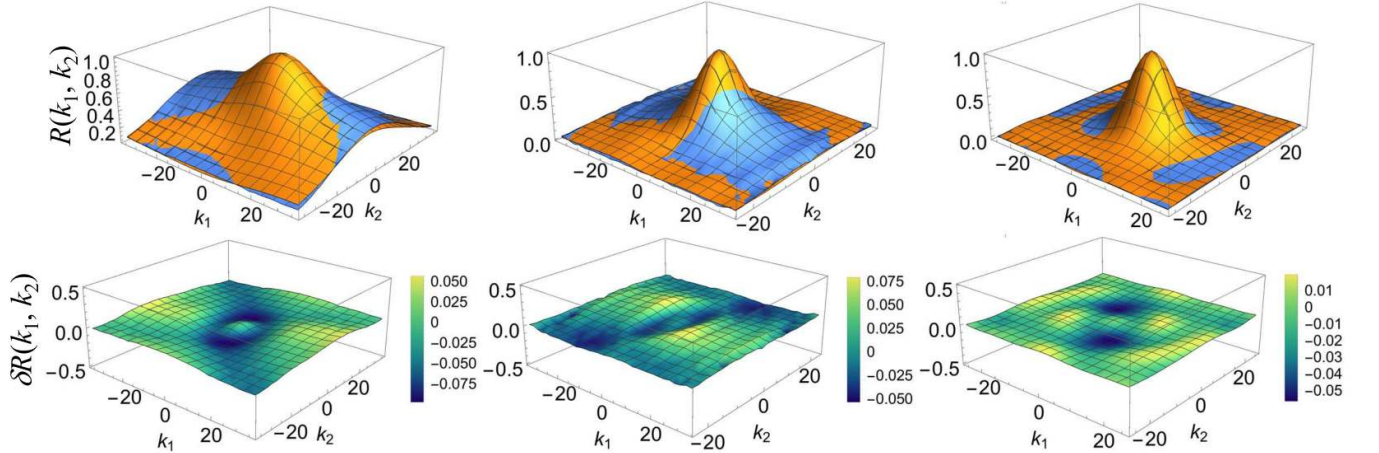


FIG. 7: Bivariate characteristic function  $R(k_1, k_2)$  obtained from the microwave data [61–63] in the frequency ranges 10-11 GHz (left), 17-18 GHz (middle) and 24-25 GHz (right). Top: Analytical result (blue) and microwave data (orange). Bottom: Difference between the two.

## Appendix B: Definition of the $\kappa$ 's

To define the  $\kappa$ 's appearing in Eq. (22) we need the following:

$$p_c^j = \frac{|\mathbf{k}|}{8} \frac{\sqrt{|\lambda_j^2 - 1|}}{(g_c^+ + \lambda_j)}, \quad j = 0, 1, 2, \quad (\text{B1})$$

$$p_c^\pm = p_c^1 \pm p_c^2, \quad (\text{B2})$$



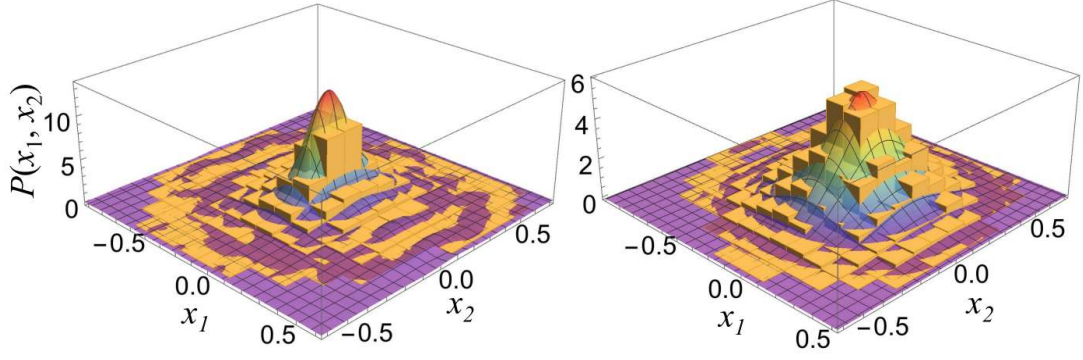


FIG. 8: Joint probability density  $P(x_1, x_2)$ , analytical (surface) and microwave data (histogram) in the frequency ranges 17-18 GHz (left) and 24-25 GHz (right).

$$q_c^+ = \frac{\mathbf{k}}{8i} \left( \frac{E}{\sqrt{4v^2 - E^2}} + ig_c^- \right) \left( \frac{1}{g_c^+ + \lambda_1} + \frac{1}{g_c^+ + \lambda_2} - \frac{2}{g_c^+ + \lambda_0} \right), \quad (\text{B3})$$

$$q_c^- = \frac{\mathbf{k}}{8i} \left( \frac{E}{\sqrt{4v^2 - E^2}} + ig_c^- \right) \left( \frac{1}{g_c^+ + \lambda_1} - \frac{1}{g_c^+ + \lambda_2} \right), \quad (\text{B4})$$

$$r_c^+ = \frac{i\mathbf{k}^*}{8} \left( \frac{E}{\sqrt{4v^2 - E^2}} - ig_c^- \right) \left( \frac{1}{g_c^+ + \lambda_1} + \frac{1}{g_c^+ + \lambda_2} - \frac{2}{g_c^+ + \lambda_0} \right), \quad (\text{B5})$$

$$r_c^- = \frac{i\mathbf{k}^*}{8} \left( \frac{E}{\sqrt{4v^2 - E^2}} - ig_c^- \right) \left( \frac{1}{g_c^+ + \lambda_1} - \frac{1}{g_c^+ + \lambda_2} \right). \quad (\text{B6})$$

It is to be noted that  $r_c^\pm = (q_c^\pm)^*$ . We also define the quantities  $l = X/Y$ ,  $m = Y/X$ ,  $\omega = 2\sqrt{XY}$ , where

$$X = 2p_a^+ + q_a^- e^{-i2\psi} + r_a^- e^{i2\psi}, \quad Y = 2p_b^+ + q_b^- e^{i2\psi} + r_b^- e^{-i2\psi}. \quad (\text{B7})$$

It can be verified that  $\omega^2$  is real for all the values of parameters involved and assumes the values from 0 to 1. The  $\kappa$ 's are given as

$$\begin{aligned} \kappa_1 &= \kappa_{11} J_1(\omega), & \kappa_2 &= \kappa_{21} J_0(\omega) + \kappa_{22} J_2(\omega), \\ \kappa_3 &= \kappa_{31} J_1(\omega) + \kappa_{32} J_3(\omega), & \kappa_4 &= \kappa_{41} J_0(\omega) + \kappa_{42} J_2(\omega) + \kappa_{43} J_4(\omega). \end{aligned} \quad (\text{B8})$$

The coefficients with the Bessel functions above are as follows

$$\kappa_{11} = -(9/8)\{p_a^+ m^{1/2}\}_+, \quad (\text{B9})$$

$$\kappa_{21} = -(1/4)(128p_a^0 p_b^0 + 14p_a^+ p_b^+ + 32p_a^- p_b^-) - \{3e^{i2\psi}(p_a^- q_b^+ + p_b^- r_a^+)\}_+ - \{e^{-4i\psi} q_a^- r_b^-\}_+, \quad (\text{B10})$$

$$\kappa_{22} = -(1/4)\{(p_a^+ p_a^+ - 4q_a^- r_a^-)m\}_+, \quad (\text{B11})$$

$$\begin{aligned} \kappa_{31} &= \left\{ -2[(p_a^+ p_a^+ + q_a^- r_a^-)m^{1/2} + 2(8p_a^0 p_b^0 + p_a^+ p_b^+ + p_a^- p_b^-)l^{1/2}](e^{i2\psi} q_b^- + e^{-i2\psi} r_b^-) \right. \\ &+ 2[(p_a^+ p_b^- + 4p_a^- p_b^+)m^{1/2} + p_b^+ p_b^- l^{1/2}](e^{-i2\psi} q_a^+ + e^{i2\psi} r_a^+) + [16p_a^0(2p_a^0 p_b^+ - 3p_b^0 p_a^+) \\ &+ 6p_a^+(q_a^+ q_b^+ + r_a^+ r_b^+) + 2p_b^+(4q_a^+ r_a^+ - q_a^- r_a^-) - 4p_a^-(p_a^+ p_b^- - 2p_a^- p_b^+) - 3p_a^+(q_a^- q_b^- + r_a^- r_b^- + p_a^+ p_b^+) \\ &- (e^{-i4\psi}/2)q_a^-(4p_a^+ r_b^- + 3p_b^+ q_a^- + 2e^{-i2\psi} q_a^- r_b^- - 8e^{i2\psi} r_a^+ r_b^+) \\ &\left. - (e^{i4\psi}/2)r_a^-(4p_a^+ q_b^- + 3p_b^+ r_a^- + 2e^{i2\psi} q_b^- r_a^- - 8e^{-i2\psi} q_a^+ q_b^+)\right]m^{1/2}\}_+, \end{aligned}$$

$$\kappa_{32} = \{p_a^+ [(p_a^+ p_a^+ + 2q_a^- r_a^-) + (3/2)(e^{-i4\psi} q_a^- q_a^- + e^{i4\psi} r_a^- r_a^-) + (2p_a^+ p_a^+ + q_a^- r_a^-)(e^{-i2\psi} q_a^- + e^{i2\psi} r_a^-)] m^{3/2}\}_+, \quad (\text{B12})$$

$$\begin{aligned} \kappa_{41} = & 32[2p_a^0 p_a^0 (p_b^- + e^{i2\psi} q_b^+) (p_b^- + e^{-i2\psi} r_b^+) + 2p_b^0 p_b^0 (p_a^- + e^{-i2\psi} q_a^+) (p_a^- + e^{i2\psi} r_a^+) \\ & + p_a^0 p_b^0 ((p_a^+ + e^{-i2\psi} q_a^-) (p_b^+ + e^{-i2\psi} r_b^-) + (p_a^+ + e^{i2\psi} r_a^-) (p_b^+ + e^{i2\psi} q_b^-))] \\ & + 256p_a^0 p_a^0 p_b^0 p_b^0 + (p_a^+ + e^{-i2\psi} q_a^-)^2 (p_b^+ + e^{-i2\psi} r_b^-)^2 + (p_a^+ + e^{i2\psi} r_a^-)^2 (p_b^+ + e^{i2\psi} q_b^-)^2 \\ & + 4[(p_a^+ + e^{-i2\psi} q_a^-) (p_b^+ + e^{i2\psi} q_b^-) - 2(p_a^- + e^{-i2\psi} q_a^+) (p_b^- + e^{i2\psi} q_b^+)] \\ & \times [(p_a^+ + e^{i2\psi} r_a^-) (p_b^+ + e^{-i2\psi} r_b^-) - 2(p_a^- + e^{i2\psi} r_a^+) (p_b^- + e^{-i2\psi} r_b^+)], \end{aligned} \quad (\text{B13})$$

$$\begin{aligned} \kappa_{42} = & -32p_a^0 p_b^0 [(p_a^+ + e^{-i2\psi} q_a^-) (p_a^+ + e^{i2\psi} r_a^-) m + (p_b^+ + e^{i2\psi} q_b^-) (p_b^+ + e^{-i2\psi} r_b^-) l] \\ & + 2[(p_a^+ + e^{-i2\psi} q_a^-) (p_b^+ + e^{i2\psi} q_b^-) - 2(p_a^- + e^{-i2\psi} q_a^+) (p_b^- + e^{i2\psi} q_b^+)] [(p_a^+ + e^{i2\psi} r_a^-)^2 m + (p_b^+ + e^{-i2\psi} r_b^-)^2 l] \\ & + 2[(p_a^+ + e^{i2\psi} r_a^-) (p_b^+ + e^{-i2\psi} r_b^-) - 2(p_a^- + e^{i2\psi} r_a^+) (p_b^- + e^{-i2\psi} r_b^+)] [(p_a^+ + e^{-i2\psi} q_a^-)^2 m + (p_b^+ + e^{i2\psi} q_b^-)^2 l], \end{aligned} \quad (\text{B14})$$

$$\kappa_{43} = \{(p_a^+ + e^{-i2\psi} q_a^-)^2 (p_a^+ + e^{i2\psi} r_a^-)^2 m^2\}_+. \quad (\text{B15})$$

In the above equations, an expression  $\mathcal{E}$  involving  $a, b, l, m, \psi$  enclosed in the bracket  $\{\}_\pm$  represents  $\{\mathcal{E}(a, b, l, m, \psi)\}_\pm := \mathcal{E}(a, b, l, m, \psi) \pm \mathcal{E}(b, a, m, l, -\psi)$ .

---